Journal of Visualized Experiments

# Effects of Adeno-associated Virus Targeting Cofilin on Electrocorticographic Recording of Cerebral Cortex Areas in Mice

--Manuscript Draft--

| | |
|---|---|
| **Article Type:** | Invited Methods Collection - JoVE Produced Video |
| **Manuscript Number:** | JoVE61976R1 |
| **Full Title:** | Effects of Adeno-associated Virus Targeting Cofilin on Electrocorticographic Recording of Cerebral Cortex Areas in Mice |
| **Corresponding Author:** | Valerie Mongrain<br>Universite de Montreal<br>Montreal, QC CANADA |
| **Corresponding Author's Institution:** | Universite de Montreal |
| **Corresponding Author E-Mail:** | valerie.mongrain@umontreal.ca |
| **Order of Authors:** | Julien DUFORT-GERVAIS |
| | Robbert HAVEKES |
| | Valerie Mongrain |
| **Additional Information:** | |
| **Question** | **Response** |
| Please specify the section of the submitted manuscript. | Neuroscience |
| Please indicate whether this article will be Standard Access or Open Access. | Open Access (US$4,200) |
| Please indicate the **city, state/province, and country** where this article will be **filmed**. Please do not use abbreviations. | Montreal, QC, Canada |
| Please confirm that you have read and agree to the terms and conditions of the author license agreement that applies below: | I agree to the Author License Agreement |
| Please provide any comments to the journal here. | |

**TITLE:**

# Effects of Adeno-associated Virus Targeting Cofilin on Electrocorticographic Recording of Cerebral Cortex Areas in Mice

**AUTHORS AND AFFILIATIONS:**

Julien DUFORT-GERVAIS[1], Robbert HAVEKES[2], Valérie MONGRAIN[1,3]

[1]Center for Advanced Research in Sleep Medicine, Recherche CIUSSS-NIM, Montreal, QC, Canada

[2]GELIFES, University of Groningen, Groningen, The Netherlands

[3]Department of Neuroscience, Université de Montréal, Montreal, QC, Canada

**CORRESPONDING AUTHOR:**

Valérie Mongrain, valerie.mongrain@umontreal.ca

**E-MAIL ADDRESSES OF CO-AUTHORS:**

Robbert Havekes, r.havekes@rug.nl

Julien Dufort-Gervais, julien.dufort-gervais@umontreal.ca

**KEYWORDS:**

Sleep regulation, motor cortex, actin severing protein, surgery, electrode, cannula, skull, neck muscle, mouse

**SUMMARY:**

This article describes a protocol for the manipulation of molecular targets in the cerebral cortex using adeno-associated viruses and for monitoring the effects of this manipulation during wakefulness and sleep using electrocorticographic recordings.

**ABSTRACT:**

The use of electrocorticographic (ECoG) recordings in rodents is relevant to sleep research and to the study of a wide range of neurological conditions. Adeno-associated viruses (AAVs) are increasingly used to improve understanding of brain circuits and their functions. AAV-mediated manipulation of specific cell populations and/or of precise molecular components has been tremendously useful to identify new sleep regulatory circuits/molecules and key proteins contributing to the adverse effects of sleep loss. For instance, inhibiting activity of the filamentous actin-severing protein, cofilin, using AAV prevents sleep deprivation-induced memory impairment. Here, a protocol has been described that combines the manipulation of cofilin function in a cerebral cortex area with the recording of ECoG activity to examine whether

cortical cofilin modulates the wakefulness and sleep ECoG recordings. AAV injection is performed during the same surgical procedure as the implantation of ECoG and electromyographic (EMG) electrodes in adult male and female mice. Mice are anesthetized, and their heads are shaved. After skin cleaning and incision, stereotaxic coordinates of the motor cortex are determined, and the skull is pierced at this location. A cannula prefilled with an AAV expressing cofilin$^{S3D}$—an inactive form of cofilin—is slowly positioned in the cortical tissue. After AAV infusion, gold-covered screws (ECoG electrodes) are screwed through the skull and cemented to the skull with gold wires inserted in the neck muscles (EMG electrodes). The animals are allowed three weeks to recover and to ensure sufficient expression of cofilin$^{S3D}$. The infected area and cell type are verified using immunohistochemistry, and the ECoG is analyzed using visual identification of vigilance states and spectral analysis. In summary, this combined methodological approach allows the investigation of the precise contribution of molecular components regulating neuronal morphology and connectivity to the regulation of synchronized cerebral cortex activity during wakefulness and sleep.

**INTRODUCTION:**

Electroencephalographic (or generally electrocorticographic [ECoG] in rodents) and electromyographic (EMG) recordings are extensively used in sleep research as well as more broadly in neuroscience, neurology, and psychiatry. In combination, these electrophysiological signals allow for the identification of vigilance states and the subsequent quantification of state duration and spectral composition, both in humans and rodents[1-4]. Such quantification has been useful to understand how sleep is modified in pathological conditions such as neurodegenerative diseases and models[5-7] or by genetic modification[8,9]. For instance, the knockout (KO) of different genes linked to neuronal communication was shown to change wakefulness and the amount of sleep in both the mouse and fruit fly[10-13]. To tackle potential developmental compensation arising from the study of full-body KO in rodents and to allow for the finest control of genetic manipulation, the use of AAVs is an efficient way to manipulate gene expression. An AAV-mediated genetic manipulation can be used to down- or upregulate a given molecular target and to restrict the manipulation to a specific cell population using different types of promoters[14]. AAVs are also extensively used as a delivery method in the clustered regularly interspaced short palindromic repeats (CRISPR)/Cas9 technology[15,16]. These methodologies allow for better temporal and spatial control of genetic manipulation, which is generally associated with the expression of a reporter permitting quantification of the infected area using immunofluorescence.

AAVs also represent the main vector for cell type-specific manipulations of neuronal activity via optogenetics and chemogenetics[17-19], which have been widely used in recent research on neurodegenerative diseases, behavior, cognition, and sleep[20-22]. In sleep research, the application of optogenetics for the activation or inhibition of certain brain regions, such as the basal forebrain, hypothalamus, and sublaterodorsal tegmentum, has been useful to determine their roles in the control of arousal, slow-wave sleep (also known as non-rapid eye movement sleep), paradoxical sleep (or rapid eye movement sleep), and cataplexy[23-25]. Furthermore, AAV-

mediated manipulations have helped elucidate important sleep regulatory circuits and molecules contributing to the adverse effects of sleep loss[26-28]. For instance, one protein shown to be implicated in sleep deprivation-induced memory impairment is cofilin[29,30]. This protein is a filamentous actin-severing protein that participates in the reorganization of actin filaments by physically binding to actin and promoting the disassembly of the filaments in a dynamic manner[31]. Inhibiting cofilin activity using an AAV-mediated approach was shown to prevent spine loss as well as synaptic plasticity and memory impairment induced by sleep deprivation in mice[29]. Collectively, these studies emphasize the usefulness and relevance of AAV-mediated manipulations to understand sleep regulation and the consequences of sleep deprivation in rodents.

Here, a protocol has been described that combines ECoG and EMG electrode implantation and recording with the manipulation of cofilin function in a cerebral cortex area of wild-type (WT) mice using an AAV. More precisely, an AAV (serotype 9) expressing the coding sequence of a phosphomimetic form of the mouse cofilin (cofilin$^{S3D}$), rendering it inactive[32,33], is injected in the motor cortex (M1 and M2). An ECoG electrode is implanted directly at the injection site to ensure recording of the synchronized cortical activity of the infected cells. The ECoG/EMG recording is conducted for 24 h under undisturbed conditions three weeks after surgery to allow for recovery, adaptation, and high cofilin$^{S3D}$ expression. The recording is then used for the identification of vigilance states and ECoG spectral analysis, as described in previous studies[11,34]. This methodology can specifically reveal how cortical cofilin modulates wakefulness and sleep ECoG in mice. This combination of electrophysiological recordings and AAV-mediated genetic manipulation is particularly relevant to investigate the roles of various molecular elements in specific brain functions and could be applied to cortical (and subcortical) brain area(s) of interest in WT and genetically modified mice of both sexes and even other species.

**PROTOCOL:**

All methods were approved by the *Comité d'éthique de l'expérimentation animale* of the Recherche CIUSSS-NIM and are in accordance with guidelines of the Canadian Council on Animal Care. See the **Table of Materials** for reagents, equipment, and materials used in this protocol.

**1. Surgery preparation**

1.1. Preparation of ECoG and EMG electrodes

1.1.1. For each animal, prepare three ECoG electrodes: using a soldering iron, place a small drop of lead-free solder on the screw cap of a gold-covered screw, and solder a 4 mm long, 0.2 mm diameter gold wire (non-insulated) on the top of the screw cap using the lead-free solder (**Figure 1A**). Prepare 2 electrodes with the gold wire straight up, and one with a 45° angle from the vertical.

1.1.2. For each animal, prepare two EMG electrodes: cut one 0.2 mm diameter gold wire to a length of 1.5 cm and a second one to 2 cm. Curve both wires for these to embrace the curve of the skull up to the neck muscles, keeping a straight end that will be soldered to the connector (**Figure 1B**).

1.1.3. For each animal, prepare one connector: use a 6-channel connector (5 mm x 8 mm x 8 mm + 3 mm metal pins), and add lead-free solder to 5 of the 6 metal pins (omitting one middle pin; **Figure 1C**). Cover the top of the connector with tape to avoid litter or water infiltration.

1.2. Preparation of AAVs and syringe pump

1.2.1. Prepare the test AAV (here, $AAV_9$-CaMKIIα0.4-cofilin$^{S3D}$-HA) and/or the control AAV (here, $AAV_9$-CaMKIIα0.4-eGFP) by diluting the stock AAV mix(es) (here, AAVs in a solution of phosphate-buffered saline containing non-ionic surfactant [0.001%]) with sterile saline to obtain the desired viral titer (generally $10^{12–13}$ genome copies [GC]/mL) and the required volume for the number of mice to be treated.

NOTE: An injected volume of 1 µL per cortical area per mouse requires the preparation of 2 µL.

1.2.2. Fix one 10 µL syringe to a syringe pump and fill it with distilled water.

1.2.3. Fill one PE50 tube of approximately 60-cm length with distilled water using a 1 mL syringe and a 21 G needle. Importantly, leave the 21G needle and syringe in place after filling. Connect the PE50 tube with the syringe pump; leave the 21 G needle/syringe on one end of the PE50 tube, and connect the other end to the 10 µL syringe.

1.2.4. Once the tube is fixed to the 10 µL syringe, remove the needle at the other end, and push the piston of the 10 µL syringe to fill the gap left by the needle with water.

NOTE: Make sure there is no air bubble, and that the tube is completely filled with water.

1.2.5. Install a 28 G cannula at the end of the tube where the needle was removed. Push water into the cannula with the 10 µL syringe to fill it completely. Fix the cannula tightly to the stereotaxic arm.

1.3. Preparation of animals

NOTE: C57BL6/J male and female mice of ~12 weeks of age were previously adapted for at least 2 weeks to housing in individual cages and to a 12-h light:12-h dark cycle with ad libitum food and water and access to a wooden cube.

1.3.1. Carefully weigh the mice, and inject intraperitoneally a mix of ketamine/xylazine (120/10 mg/kg) for anesthesia. Wait approximately 10 min for deep anesthesia.

1.3.2. Shave the hair from the back of the ears to the front of the head between the eyes using a hair trimmer.

NOTE: Be very careful not to cut the whiskers (protect the whiskers with a finger during shaving) as whisker trimming will modify sensory inputs and ECoG activity[35,36].

1.3.3. Add a generous drop of ophthalmic ointment on each eye to prevent dehydration. Verify the depth of anesthesia regularly during the procedure by pinching a toe from the hind paw. Provide the mouse with 0.5–1.5% isoflurane to ensure deep anesthesia if a toe pinch reflex appears.

**2. Intracortical AAV injection with a syringe pump**

NOTE: Perform all the following steps with sterilized instruments and in a clean environment. Use 70% ethanol to further wash sterilized instruments and to wash electrodes prepared in section 1.1 as well as anchor screws (non-gold-covered screws) before beginning the surgery.

2.1. Carefully fix the head of the mouse on the stereotaxic apparatus with ear bars.

NOTE: Make sure the head is not moving laterally, and fix the nose of the mouse on the stereotaxic adapter.

2.2. Gently pull the tongue of the animal out of the mouth to avoid suffocation. Monitor the breathing frequently during the procedure.

2.3. Sterilize the shaved area of the head with 70% ethanol and by holding the skin with an extra fine Graefe forceps, cut the skin from the base of the ears to the level of the eyes with tissue scissors. Use four surgical clamps to stretch the skin and expose the skull (two on each side of the incision; see **Figure 1D**).

2.4. Scratch the skull surface with a sharp scissor tip, and while avoiding bone sutures, remove the periosteum and create overlapping streaks in two or more directions. Remove the bone fragments, and dry the skull with 70% ethanol.

NOTE: The scratching and the streaking will help make the recording montage more robust by improving the adherence of the cement to the skull (see below).

2.5. With the cannula fixed to the stereotaxic arm, identify the location of the bregma (i.e., the intersection between the skull coronal and sagittal sutures; **Figure 1D**) and lambda (i.e., the intersection between the skull sagittal suture and a straight line connecting the left and right lambdoid suture; **Figure 1D**), and note the stereotaxic coordinates of each. If the difference in z coordinates (vertical axis) of the bregma and lambda is greater than 0.3 mm, adjust the height of the nose using the stereotaxic adapter until the z position of bregma and lambda are aligned.

2.6. Mark the position of the cannula on the skull with a pen at these coordinates (motor cortex): 1.5 mm lateral right to midline and 1.5 mm anterior to bregma. Carefully pierce the skull at the position of the cannula with a 0.7 mm drill bit in a direction perpendicular to the skull surface (aligned with the vertical axis). Wash the pierced skull with a sterile cotton tip impregnated with a 10% providone-iodine solution.

2.7. Load the cannula with a 1 µL air bubble by pulling the 10 µL syringe piston back by 1 µL. Load the test AAV (here $AAV_9$-CaMKIIα0.4-Cofilin$^{S3D}$-HA) or the control AAV (here $AAV_9$-CaMKIIα0.4-eGFP) into the cannula previously loaded with the air bubble: mix the AAV by slowly pipetting up and down, and pipet 1.7 µL on a sterile Petri dish. Then, aspirate 1.5 µL of the solution in the cannula by slowly pulling the piston of the 10 µL syringe.

2.8. Mark the position of the air bubble on the PE50 tube to allow the tracking of the injection. Align the cannula with the hole on the skull for the vertical position of the cannula to reach the upper edge of the skull (i.e., skull surface). From the skull surface, slowly lower the cannula by 1.5 mm (to reach 1.5 mm below skull surface and layer V of the motor cortex).

NOTE: Be very careful not to lower the cannula too much to avoid unnecessary lesion of the brain tissue.

2.9. Start the syringe pump to inject 1 µL of AAV over the course of 40 min (speed: 0.025 µL/min to minimize tissue damage). Keep track of the injection on the PE50 tube with the movement of the air bubble, and make the necessary adjustments.

2.10. After the injection is completed, leave the cannula in place for 5 min to ensure sufficient diffusion and avoid backflow. Then, slowly and carefully lift the stereotaxic arm to remove the cannula from the cortex.

**3. ECoG/EMG electrode implantation**

3.1. Using straight Kelly forceps, slowly screw one ECoG electrode (with straight gold-wire) in the vertical axis (same angle that the hole was pierced) in the hole where the AAV was injected. Leave at least 2.5 mm of the screw out of the skull to minimize damage to the dura and cerebral cortex (i.e., for an approximate depth of 1.1 mm from the skull surface; **Figure 1D**).

3.2. Mark the position of the posterior ECoG electrode and the reference electrode on the skull with a pen at these coordinates: posterior electrode (visual cortex) 1.5 mm lateral right to midline and 1.5 mm anterior to lambda, reference electrode (somatosensory cortex) 2.6 mm lateral right to midline and 0.7 mm posterior to bregma. Also, mark the position of three maintenance screws (acting as anchors between the skull and dental cement to solidify head montage) on the left hemisphere with no specific coordinates, but as distant as possible from each other and from the ECoG electrodes.

3.3. Carefully pierce the skull at the marked position of the other electrodes and anchor screws with the 0.7 mm drill bit. Pierce in a direction perpendicular to the skull surface for each screw (i.e., vertical axis for the posterior electrode but with an angle from the vertical axis for other sites). Wash the pierced skull with a 10% providone-iodine solution, and block the holes with small, rolled pieces of delicate task wipers before installing the screws to prevent bleeding and contamination.

3.4. Using the straight Kelly forceps, fasten the maintenance screws in the left hemisphere and then fasten the last two electrodes in the right hemisphere. Make sure to screw with the same angle that the holes were pierced and to leave at least 2.5 mm of each screw sticking out of the skull (**Figure 1D**).

NOTE: To maximize the solidity of the final montage and the quality of the electrophysiological signals, be careful not to touch any screw when installing the next one.

3.5. Place a few small drops of dental cement in the center of the ring-like space inside the screws. Insert the curved end of one EMG electrode (prepared at step 1.1.2) up to approximately 1–2 mm in the neck muscles by holding the curved extremity using Dumont #5 forceps and lifting the skin above muscles with extra-fine Graefe forceps. Then, place the curved side and elbow of the electrode in the dental cement; repeat for the second EMG electrode.

NOTE: The straight end of the longer EMG electrode should be aligned with the anterior ECoG electrode and that of the shorter EMG electrode with the posterior ECoG electrode. Make sure the two EMG electrodes are not touching each other or any of the screws.

3.6. Cover the eyes of the mice, and apply light for 3–5 min to help cement solidification. Once the EMG electrodes are holding firmly, cover the base of the ECoG electrodes, and anchor the screws with dental cement to form a crown-shaped contour. Cover the eyes of the mice, and apply light for 3–5 min to help cement solidification.

NOTE: Do not apply cement on the ECoG and EMG electrode extremities (gold wire that will be soldered to the connector) or on the skin.

3.7. Fill the center of the montage with previously mixed acrylic cement. During cement solidification, remove the four surgical clamps holding the skin (and wash these immediately with delicate task wipers).

NOTE: Do not apply cement on the ECoG and EMG electrode extremities (gold wire that will be soldered to the connector) or on the skin.

3.8. Suture the skin at the back and the front of the montage so that the skull is not exposed (but avoid stretching the skin too much) using a suture needle (13 mm 3/8 c) and synthetic absorbable monofilament.

3.9. Hold the connector above the montage with curved forceps, and carefully align the gold wire of electrodes with the connector pins. Solder electrode extremities to connector pins with the soldering iron.

NOTE: Proceed quickly to avoid overheating and damage to the cortical tissue. Make sure that each electrode makes good contact with the corresponding connector pin, and that the electrodes are not connected to each other.

3.10. Remove the mouse from the stereotaxic frame. Cover the empty space between the connector and the head with previously mixed acrylic cement by covering all connections between electrodes and connector pins.

NOTE: Avoid cement infiltration inside the connector by holding the mouse with the connector above the head (head straight not leaning).

3.11. Weigh the mouse and place it in a clean cage (preferably equipped with a non-meshed lid) on a heat pad (individual housing to avoid damage to the head montage). Monitor the animal regularly, and administer 0.1 mg/kg of buprenorphine subcutaneously upon awakening, and 12 h later if the animal shows signs of pain (e.g., abnormal posture, squinted eyes).

NOTE: Weight gain relative to pre-surgery weight should not exceed 1.5 g.

**4. Recordings**

4.1. House mice individually to avoid damage to the head montage as a result of mutual grooming as well as damage and entanglement of the recording cables.

NOTE: For this protocol, mice were housed with ad libitum access to food, water, and a wooden cube, and daily monitoring was conducted.

4.2. Connect the mice to recording cables 2 weeks after surgery for adaptation to cabling conditions.

4.3. Record ECoG/EMG signals for 24 h (or longer/shorter depending on research questions).

NOTE: ECoG/EMG signal recording was accomplished using a cable, a swivel connector (to allow rotation of the cable), a 36-channel wearable box, and an amplifier, which was connected to a computer. Signals are sampled at 256 Hz (or more depending on research questions) and recorded with commercial software (see the **Table of Materials**). To ensure sufficient viral expression, experiments should be done at least 3 weeks after AAV injection, as described previously[29,37].

4.4. After recording, sacrifice the mice by cervical dislocation (or other methods depending on

the immunostaining protocol), and harvest the brain for immunostaining.

**REPRESENTATIVE RESULTS:**

After electrophysiological recordings, immunofluorescence is used to define the area infected by the AAV injection and to validate the expression of cofilin$^{S3D}$ (**Figure 2**). Immunostaining can be performed using a methodology similar to what has been described previously[29,37-39]. The AAV expresses an inactive form of cofilin fused with a hemagglutinin (HA)-Tag (cofilin$^{S3D}$-HA), which is detected by immunofluorescence using an anti-HA antibody and a secondary antibody (Alexa Fluor 488). The infected excitatory neurons (here, targeted with a calcium/calmodulin-dependent protein kinase II [*CamKII*$\alpha$] promoter controlling the expression of the transgene contained in the AAV) are stained with the anti-HA antibody. A successful infection is indicated by the staining of the neurons in the motor cortex surrounding the injection site (**Figure 2A,B**). In this representative example, the cerebral cortex of the other hemisphere did not show any noticeable staining. Nonetheless, given that excitatory neurons can project to distant brain areas, staining in the contralateral hemisphere is not necessarily an indication of unsuccessful injection. Higher magnification of the infected area showed staining of cell bodies and projections, confirming that only specific cells of the targeted cortical area were infected (**Figure 2C**).

Co-staining with markers of excitatory neurons (e.g., vesicular glutamate transporter 1, CaMKII$\alpha$) can also be performed to validate cell type-specificity. In addition, co-staining with markers of inhibitory neurons or astrocytes can be performed in case these cells are targeted using different promoters. Co-staining of cofilin$^{S3D}$-HA and CaMKII$\alpha$ was also performed in the same animal for an area more posterior to the injection site that still showed anti-HA staining in the motor cortex (**Figure 2D**). The higher magnification image of the area shows cells clearly expressing cofilin$^{S3D}$-HA (Alexa Fluor 488, **Figure 2E**) and CaMKII$\alpha$ (Alexa Fluor 568, **Figure 2F**). The superposition of the cofilin$^{S3D}$-HA and CaMKII$\alpha$ staining reveals that most (if not all) cells stained for cofilin$^{S3D}$-HA are also positive for CaMKII$\alpha$ (**Figure 2G**). This observation supports the specificity of the infection for excitatory neurons.

To assess the impact of cofilin manipulation on ECoG activity, ECoG and EMG signals are used to perform a visual identification of vigilance states (wakefulness, slow wave sleep, paradoxical sleep). This is done on 4-s epochs because of the rapid change in vigilance state in the mouse[2], and here, for a full 24-h recording. Standard analyses include computation of sleep architecture and spectral analysis variables, as conducted previously for different datasets[11-13,28,34]. In particular, spectral analysis of the ECoG signal of the different states will index state composition and quality. To remove differences that could arise, for instance, from different depths of the electrodes, spectral analysis data can be expressed relative to the total power of all states of a given animal (**Figure 3A**). Given the very low relative amplitude of ECoG activity in higher frequencies, relative power spectra for wakefulness, slow wave sleep, and paradoxical sleep have been log-transformed to more adequately visualize and simultaneously compare the

activity in low and high frequencies. This analysis indicates state-specific differences in spectral activity under conditions of cofilin inactivation (**Figure 3B**). More precisely, these preliminary findings combining male and female mice point out that cofilin inactivation significantly increases spectral power in fast frequencies (14–30 Hz) during wakefulness and in slow frequencies (1–4 Hz) during paradoxical sleep, while leaving ECoG activity during slow-wave sleep mainly unaffected. In addition, cofilin inactivation appears to increase inter-mouse variability in ECoG activity (particularly noticeable from error bars for wakefulness in **Figure 3B**).

**FIGURE LEGENDS:**

**Figure 1**: **Preparation of ECoG/EMG montage components and representative example of ECoG electrode placement.** (**A**) An ECoG electrode: a 4 mm long, 0.2 mm diameter gold wire (non-insulated) is fused on the head of a gold-covered screw (1.9 mm head diameter, 1.14 mm thread major diameter, 3.6 mm total length) using lead-free solder. (**B**) EMG electrodes: two gold wires (1.5 and 2 cm) are curved to embrace the curve of the skull up to the neck muscle, and the other end is kept straight to be soldered to the connector. (**C**) A 6-channel connector: lead-free solder is added to 5 of the 6 metal pins (omitting one in the middle) of the connector (5 mm x 8 mm x 8 mm + 3 mm metal pins). The top of the connector is covered with tape to avoid litter/water infiltration. (**D**) Example of the positioning of the three maintenance screws on the skull of the left hemisphere and of the three ECoG electrodes (including a reference electrode) on the right hemisphere. The precise stereotaxic coordinates of the ECoG electrodes are indicated in steps 2.6 and 3.2 and have been calculated according to the location of the bregma and lambda (which are indicated by the yellow dots). Abbreviations: ECoG = electrocorticographic; EMG = electromyographic.

**Figure 2**: **Representative immunostaining to define the AAV-infected area and cell type.** (**A**) Schematic representation showing the injection site of the coronal slice presented in panel B. The position is 1.1 mm anterior to the bregma, and the cannula (shown in red) was targeted to layers V of the right primary motor cortex (M1). Representation modified from Franklin and Paxinos[40]. (**B**) Immunostaining of HA to detect cofilin$^{S3D}$-HA expression in neurons shown for a coronal slice of the full brain located approximately 1.1 mm anterior to the bregma. The infected area mainly localizes to layers V and VI (infragranular layers) of the right primary and secondary motor cortices (M1 and M2). Scale bar = 500 µm. The square represents the area shown in C. (**C**) Higher magnification of the infected area showing staining of infected cells and confirming expression of cofilin$^{S3D}$-HA in deeper layers of the motor cortex. Scale bar = 100 µm. (**D**) Co-immunostaining of HA and CaMKIIα to assess cell type-specificity shown for a coronal slice of the right hemisphere located approximately 0.5 mm anterior to bregma and therefore, posterior to the injection site (same mouse as in panels B and C). The infected area localizes to motor cortices (M1 and mainly M2). Scale bar = 500 µm. The square represents the area shown in E, F, and G. (**E**) Higher magnification of the infected area showing staining of infected cells and confirming expression of cofilin$^{S3D}$-HA. Scale bar = 100 µm. (**F**) Higher magnification of the infected area showing staining of CaMKIIα-positive cells. Scale bar = 100 µm. (**G**) Higher magnification of the infected area showing co-labeling of cofilin$^{S3D}$-HA and CaMKIIα, confirming

that infected cells are CaMKIIα-positive. Scale bar = 100 µm. Abbreviations: AAV; M1 = primary motor cortex; M2 = secondary motor cortex; V and VI = infragranular layers; CPu = caudate putamen (striatum); LV = lateral ventricle; HA= hemagglutinin; CamKIIα = calcium/calmodulin-dependent protein kinase II alpha.

**Figure 3**: **Representative power spectra for wakefulness, slow wave sleep, and paradoxical sleep obtained after viral manipulation of cofilin function.** Male (n = 5 per group) and female (n = 2 per group) mice injected with $AAV_9$-CaMKIIα0.4-cofilin$^{S3D}$-HA (viral titer $2.58 \times 10^{13}$ GC/mL) or with a control AAV ($AAV_9$-CaMKIIα0.4-eGFP $1.25 \times 10^{13}$ GC/mL; half of the test titer to control for the enhanced signal of this control AAV) in layer V of the motor cortex were recorded for 24 h, and the electrocorticographic signal was subjected to spectral analysis (fast Fourier Transform to calculate spectral power between 0.5 and 30 Hz with a 0.25-Hz resolution). (**A**) Power spectra during the three vigilance states expressed relative to total power of all states. (**B**) Relative power spectra log-transformed to more adequately represent group differences in higher frequencies. The suppression of cofilin activity in the motor cortex using $AAV_9$-CaMKIIα0.4-cofilin$^{S3D}$-HA significantly increases electrocorticographic activity in the beta range (14–30 Hz) during wakefulness, and in the delta range (1–4 Hz) during paradoxical sleep in comparison to control injections (red lines above x axes indicate Mann-Whitney *U*-test on frequency band power $p < 0.05$). Abbreviations: AAV; V = infragranular layer; GC = genome copies; HA= hemagglutinin; CamKIIα = calcium/calmodulin-dependent protein kinase II alpha; eGFP = enhanced green fluorescent protein.

**DISCUSSION:**

This protocol describes a precise and straightforward method to monitor ECoG and EMG activity during the manipulation of molecular targets using AAVs. For adequate between-group comparison, it is highly recommended to always plan surgical procedures (AAV injection and electrode implantation) on the same day for test and control animals, and to record their electrophysiological signals simultaneously. To obtain similar viral expression between the test and control animals, injecting the same viral titer is desirable. In the present case, viral titer of control AAV had been decreased to half of the test AAV to ensure similar viral expression. Experimenters should be very careful with measurements of stereotaxic coordinates to ensure low between-animal variability in brain area/cortical layer targeting. Additionally, given that the injection depth is calculated from the skull surface, and that skull thickness varies with age and sex, the placement of the cannula should always be verified using post-protocol histology or immunohistochemistry (e.g., **Figure 2**) to ensure adequate positioning/depth of injection, and the stereotaxic coordinates should be adjusted if necessary. Throughout the 40-min AAV injection, it is very important to monitor the injection speed to rapidly detect and correct potential issues such as pump blockage. Some experimental steps are also crucial to obtain optimal electrophysiological signals. For instance, do not drive the screws in too far during electrode implantation; screws should stick out of the skull by at least 2.5 mm to minimize damage to the cerebral cortex and the formation of a glial scar. Afterwards, it is also tremendously important to i) avoid applying cement to the extremities of the electrodes, ii)

ensure a rapid soldering of the electrodes to the connector, and iii) make sure that there is no contact between the electrodes.

The procedure presented here for ECoG and EMG recording is extremely well established, simple, and widely used to monitor wakefulness and sleep in mice[2,11,13,34]. Continuous ECoG and EMG recordings can be performed for several consecutive days (and even weeks) to generate a very rich dataset that can be used to perform several lines of analysis comprising variables related to wakefulness and sleep amount and architecture[2,11,12] (e.g., time spent in different states per light and dark periods, number of episodes of each state, 24-h distribution of sleep), wakefulness and sleep spectral content[34,41] (e.g., power in different frequency bands [similar to **Figure 3**], scale-free activity), and characteristics of individual waves[42-44] (e.g., slow-wave amplitude and slope). When used in combination with AAV-mediated molecular manipulations, an additional advantage is the avoidance of potential developmental compensation that can occur in transgenic animals. With practice, the whole procedure, including the 40-min AAV injection, can be performed in approximately 90 min. Mortality rate should be (very) low as the surgery is minimally invasive.

The simultaneous use of ECoG/EMG recording and targeted manipulation with AAV offers a variety of other advantages and applications. For instance, the precision of stereotaxic targeting, when adequately performed, is very high and replicable and is useful to determine the specific role of a given brain region (and/or a cell type or a molecular element within the region) in the regulation of sleep or other physiological processes. Several different cortical areas can thus be easily targeted using adaptations of the current protocol. Moreover, target manipulations using AAVs could be directed to a cortical/subcortical area different from the ECoG recording sites. In such cases, the burr hole for AAV injection could be covered by a small glass coverslip fixed using dental cement (or bone wax). For enhanced specificity, the AAV construction often includes a promoter that allows targeted infection of a precise cell type[14]. A *CamKIIα* promoter was used in the present protocol to specifically target excitatory pyramidal cells[14,29,45] of the motor cortex. This strategy has enabled the inactivation of cofilin (using cofilin$^{S3D}$)[32,33] in excitatory neurons of the motor cortex and the observation of state-specific changes in ECoG activity (**Figure 3**). To assess infection/transduction efficacy, future protocol users could combine the presented AAV-ECoG protocol with one of co-staining by immunofluorescence, and use high magnification images to calculate the number of cells showing double-labeling out of the total number of cells showing single-labeling of the target (here, CaMKII$\alpha$-expressing neurons). In a recent study, an AAV-ECoG method similar to the one described here was used to overexpress fragile X mental retardation syndrome-related protein 1 (FXR1) in all neurons of the motor cortex using an AAV containing a synapsin promoter and revealed an effect of this manipulation on vigilance state distribution and spectral content[28]. These findings illustrate how manipulating a given molecule in a target brain region using AAVs can reveal roles in the regulation of specific wakefulness/sleep parameters.

A limitation of the described protocol is the small lesion of brain tissue occurring with cannula placement before performing the AAV injection, which could also be accompanied by an inflammatory response. This could be of particular concern when performing AAV injection in

subcortical areas and should always be tackled by using adequate controls. Alternatively, the current protocol could be followed by the quantification of reactive gliosis and/or of microglial activation (e.g., using immunofluorescence) to ensure similar levels in control and test groups and therefore, on the ECoG readout. A second limitation relates to the risk of bad connection between an electrode and the connector, which could result in a continuously or occasionally bad electrophysiological signal. Solidly screwed, soldered, and cemented electrodes will minimize the incidence of this issue. A third limitation is related to animals being tethered via the head montage during the recording, which could limit locomotion and other behaviors, at least to some extent, and occasionally result in cabling damage and signal loss. Finally, the presented protocol is more suitable for adult mice, given that the skull size of younger animals may cause difficulties in installing the depicted head montage, as described previously[2].

Combined ECoG/EMG recording and AAV-mediated manipulation of a precise target is also applicable to research fields other than the neuroscience of sleep. It could be used to study and manipulate epileptic events in animal models of seizure and is a powerful tool to modulate brain oscillations involved in memory encoding and consolidation[46,47]. Accordingly, potential applications certainly encompass the fields of fundamental research in psychiatry and neurology, including neurodegenerative diseases. In addition to the capacity of expressing an inactive form of a molecule, AAVs can and have been used to overexpress or downregulate (e.g., small-interfering RNA, CRISPR/Cas9) or to rescue the expression of a molecule in a full-body KO. Importantly, the dual methodology of the current protocol is also applicable to other mammalian species such as rats and diurnal rodents that represent interesting models to understand both sleep and neurodegeneration[48,49].

**ACKNOWLEDGMENTS:**

The work was funded by the Canada Research Chair in Sleep Molecular Physiology. The authors are thankful to Chloé Provost and Caroline Bouchard for technical help.

**DISCLOSURES:**

The authors have nothing to disclose.

**REFERENCES:**

1. Campbell, I. G. EEG recording and analysis for sleep research. *Current Protocols in Neuroscience.* **Chapter 10** (unit 10.2) (2009).
2. Mang, G. M., Franken P. Sleep and EEG phenotyping in mice. *Current Protocols in Mouse Biology*. **2** (1), 55–74 (2012).
3. Bastien, C.H. et al. Insomnia and sleep misperception. *Pathologie Biologie.* **62** (5), 241–251 (2014).

4. Malafeev, A. et al. Automatic artefact detection in single-channel sleep EEG recordings. *Journal of Sleep Research.* **28** (2), e12679 (2019).
5. Latreille, V. et al. Electroencephalographic prodromal markers of dementia across conscious states in Parkinson's disease. *Brain.* **139** (Pt 4), 1189–1199 (2016).
6. Rodrigues Brazete, J. et al. Electroencephalogram slowing predicts neurodegeneration in rapid eye movement sleep behavior disorder. *Neurobiology of Aging.* **37**, 74–81 (2016).
7. Kent, B. A., Strittmatter, S. M., Nygaard, H. B. Sleep and EEG power spectral analysis in three transgenic mouse models of Alzheimer's disease: APP/PS1, 3xTgAD, and Tg2576. *Journal of Alzheimers Disease.* **64** (4), 1325–1336 (2018).
8. Chang, A. M. et al. Circadian gene variants influence sleep and the sleep electroencephalogram in humans. *Chronobiology International.* **33** (5), 561–573 (2016).
9. Shi, G., Wu, D., Ptacek, L. J., Fu, Y. H. Human genetics and sleep behavior. *Current Opinion in Neurobiology.* **44**, 43–49 (2017).
10. Nakai, Y. et al. Calcineurin and its regulator sra/DSCR1 are essential for sleep in Drosophila. *Journal of Neuroscience.* **31** (36), 12759–12766 (2011).
11. El Helou, J. et al. Neuroligin-1 links neuronal activity to sleep-wake regulation. *Proceedings of the National Academy of Sciences of the United States of America*. **110** (24), 9974–9979 (2013).
12. Freyburger, M. et al. EphA4 is involved in sleep regulation but not in the electrophysiological response to sleep deprivation. *Sleep.* **39** (3), 613–624 (2016).
13. Seok, B. S. et al. The effect of Neuroligin-2 absence on sleep architecture and electroencephalographic activity in mice. *Molecular Brain.* **11** (1), 52 (2018).
14. Haery, L. et al. Adeno-associated virus technologies and methods for targeted neuronal manipulation. *Frontiers in Neuroanatomy.* **13**, 93 (2019).
15. Schmidt, F., Grimm, D. CRISPR genome engineering and viral gene delivery: a case of mutual attraction. *Biotechnology Journal.* **10** (2), 258–272 (2015).
16. Wang, D., Zhang, F., Gao, G. CRISPR-based therapeutic genome editing: strategies and in vivo delivery by AAV vectors. *Cell.* **181** (1), 136–150 (2020).
17. Havekes, R. et al. Transiently increasing cAMP levels selectively in hippocampal excitatory neurons during sleep deprivation prevents memory deficits caused by sleep loss. *Journal of Neuroscience.* **34** (47), 15715–15721 (2014).
18. Fuller, P. M., Yamanaka, A., Lazarus, M. How genetically engineered systems are helping to define, and in some cases redefine, the neurobiological basis of sleep and wake. *Temperature (Austin).* **2** (3), 406–417 (2015).
19. Naso, M. F., Tomkowicz, B., Perry, W. L.3rd, Strohl W. R. Adeno-associated virus (AAV) as a vector for gene therapy. *BioDrugs.* **31** (4), 317–334 (2017).
20. Ono, D., Yamanaka, A. Hypothalamic regulation of the sleep/wake cycle. *Neuroscience Research.* **118**, 74–81 (2017).
21. Shiromani, P. J., Peever, J. H., New neuroscience tools that are identifying the sleep-wake circuit. *Sleep.* **40** (4), zsx032 (2017).
22. Oishi, N. et al. Artificial association of memory events by optogenetic stimulation of hippocampal CA3 cell ensembles. *Molecular Brain.* **12** (1), 2 (2019).
23. Anaclet, C. et al. Genetic activation, inactivation, and deletion reveal a limited and nuanced role for somatostatin-containing basal forebrain neurons in behavioral state control. *Journal of*

615 *Neuroscience.* **38** (22), 5168–5181 (2018).
616 24. Chen, K.S. et al. A hypothalamic switch for REM and non-REM sleep. *Neuron.* **97** (5), 1168–
617 1176.e4 (2018).
618 25. Torontali, Z. A., Fraigne, J. J., Sanghera, P., Horner, R., Peever, J. The sublaterodorsal
619 tegmental nucleus functions to couple brain state and motor activity during REM sleep and
620 wakefulness. *Current Biology.* **29** (22), 3803–3813.e5 (2019).
621 26. Rolls, A. et al. Optogenetic disruption of sleep continuity impairs memory consolidation.
622 *Proceedings of the National Academy of Sciences of the United States of America*. **108** (32),
623 13305–13310 (2011).
624 27. Ognjanovski, N., Broussard, C., Zochowski, M., Aton, S. J. Hippocampal network oscillations
625 rescue memory consolidation deficits caused by sleep loss. *Cerebral Cortex.* **28** (10), 3711–3723
626 (2018).
627 28. Khlghatyan, J. et al. Fxr1 regulates sleep and synaptic homeostasis. *EMBO Journal.* **39** (21),
628 e103864 (2020).
629 29. Havekes, R. et al. Sleep deprivation causes memory deficits by negatively impacting
630 neuronal connectivity in hippocampal area CA1. *Elife.* **5**, e13424 (2016).
631 30. Wong, L. W., Tann, J. Y., Ibanez, C. F., Sajikumar, S. The p75 neurotrophin receptor is an
632 essential mediator of impairments in hippocampal-dependent associative plasticity and
633 memory induced by sleep deprivation. *Journal of Neuroscience*. **39** (28), 5452–5465 (2019).
634 31. Mizuno, K. Signaling mechanisms and functional roles of cofilin phosphorylation and
635 dephosphorylation. *Cellular Signalling.* **25** (2), 457–469 (2013).
636 32. Nagaoka, R., Abe, H., Obinata T. Site-directed mutagenesis of the phosphorylation site of
637 cofilin: its role in cofilin-actin interaction and cytoplasmic localization. *Cell Motility and the*
638 *Cytoskeleton.* **35** (3), 200–209 (1996).
639 33. Elam, W.A. et al. Phosphomimetic S3D cofilin binds but only weakly severs actin filaments.
640 *Journal of Biological Chemistry.* **292** (48), 19565–19579 (2017).
641 34. Areal, C. C., Cao, R., Sonenberg, N., Mongrain, V. Wakefulness/sleep architecture and
642 electroencephalographic activity in mice lacking the translational repressor 4E-BP1 or 4E-BP2.
643 *Sleep.* **43** (2), zsz210 (2020).
644 35. Vyazovskiy, V., Borbely, A.A., Tobler, I. Unilateral vibrissae stimulation during waking
645 induces interhemispheric EEG asymmetry during subsequent sleep in the rat. *Journal of Sleep*
646 *Research.* **9** (4), 367-371 (2000).
647 36. Sitnikova, E. Neonatal sensory deprivation promotes development of absence seizures in
648 adult rats with genetic predisposition to epilepsy. *Brain Research.* **1377**, 109–118 (2011).
649 37. Tudor, J. C. et al. Sleep deprivation impairs memory by attenuating mTORC1-dependent
650 protein synthesis. *Science Signaling.* **9** (425), ra41 (2016).
651 38. Evilsizor, M. N., Ray-Jones, H. F., Lifshitz, J., Ziebell, J. Primer for immunohistochemistry on
652 cryosectioned rat brain tissue: example staining for microglia and neurons. *Journal of Visualized*
653 *Experiments*. (99), e52293 (2015).
654 39. Dufort-Gervais, J. et al. Neuroligin-1 is altered in the hippocampus of Alzheimer's disease
655 patients and mouse models, and modulates the toxicity of amyloid-beta oligomers. *Scientific*
656 *Reports*. **10** (1), 6956 (2020).
657 40. Franklin, K. B. J., Paxinos, G. The mouse brain in stereotaxic coordinates, Third edition.
658 Academic Press, New York (2007).

41. Lina, J. M., O'Callaghan, E. K., Mongrain, V. Scale-free dynamics of the mouse wakefulness and sleep electroencephalogram quantified using Wavelet-Leaders. *Clocks & Sleep.* **1** (1), 50–64 (2019).
42. Massart, R. et al. The genome-wide landscape of DNA methylation and hydroxymethylation in response to sleep deprivation impacts on synaptic plasticity genes. *Translational Psychiatry.* **4**, e347 (2014).
43. Freyburger, M., Poirier, G., Carrier, J., Mongrain, V. Shorter duration of non-rapid eye movement sleep slow waves in EphA4 knockout mice. *Journal of Sleep Research.* **26** (5), 539–546 (2017).
44. Hubbard, J. et al. Rapid fast-delta decay following prolonged wakefulness marks a phase of wake-inertia in NREM sleep. *Nature Communications.* **11** (1), 3130 (2020).
45. Johansen, J. P. et al. Optical activation of lateral amygdala pyramidal cells instructs associative fear learning. *Proceedings of the National Academy of Sciences of the United States of America*. **107** (28), 12692–12697 (2010).
46. Boyce, R., Glasgow, S. D., Williams, S., Adamantidis, A. Causal evidence for the role of REM sleep theta rhythm in contextual memory consolidation. *Science.* **352** (6287), 812–816 (2016).
47. Bandarabadi, M. et al. Dynamic modulation of theta-gamma coupling during rapid eye movement sleep. *Sleep.* **42** (12), zsz182 (2019).
48. Estrada, C. et al. Transcranial magnetic stimulation and aging: Effects on spatial learning and memory after sleep deprivation in Octodon degus. *Neurobiology of Learning and Memory.* **125**, 274–281 (2015).
49. Hurley, M. J. et al. The long-lived Octodon degus as a rodent drug discovery model for Alzheimer's and other age-related diseases. *Pharmacology & Therapeutics.* **188**, 36–44 (2018).

Figure 1



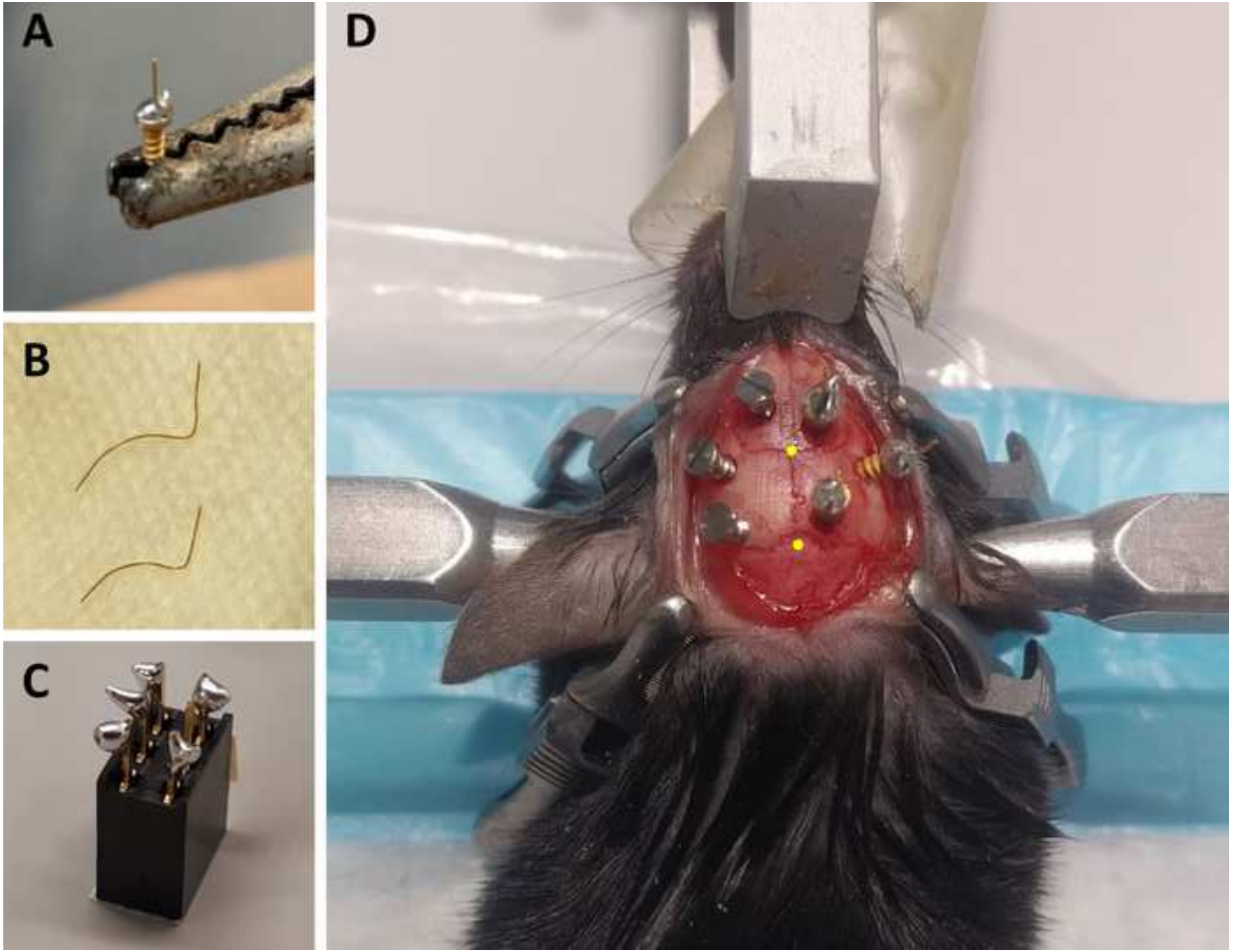

Figure 2



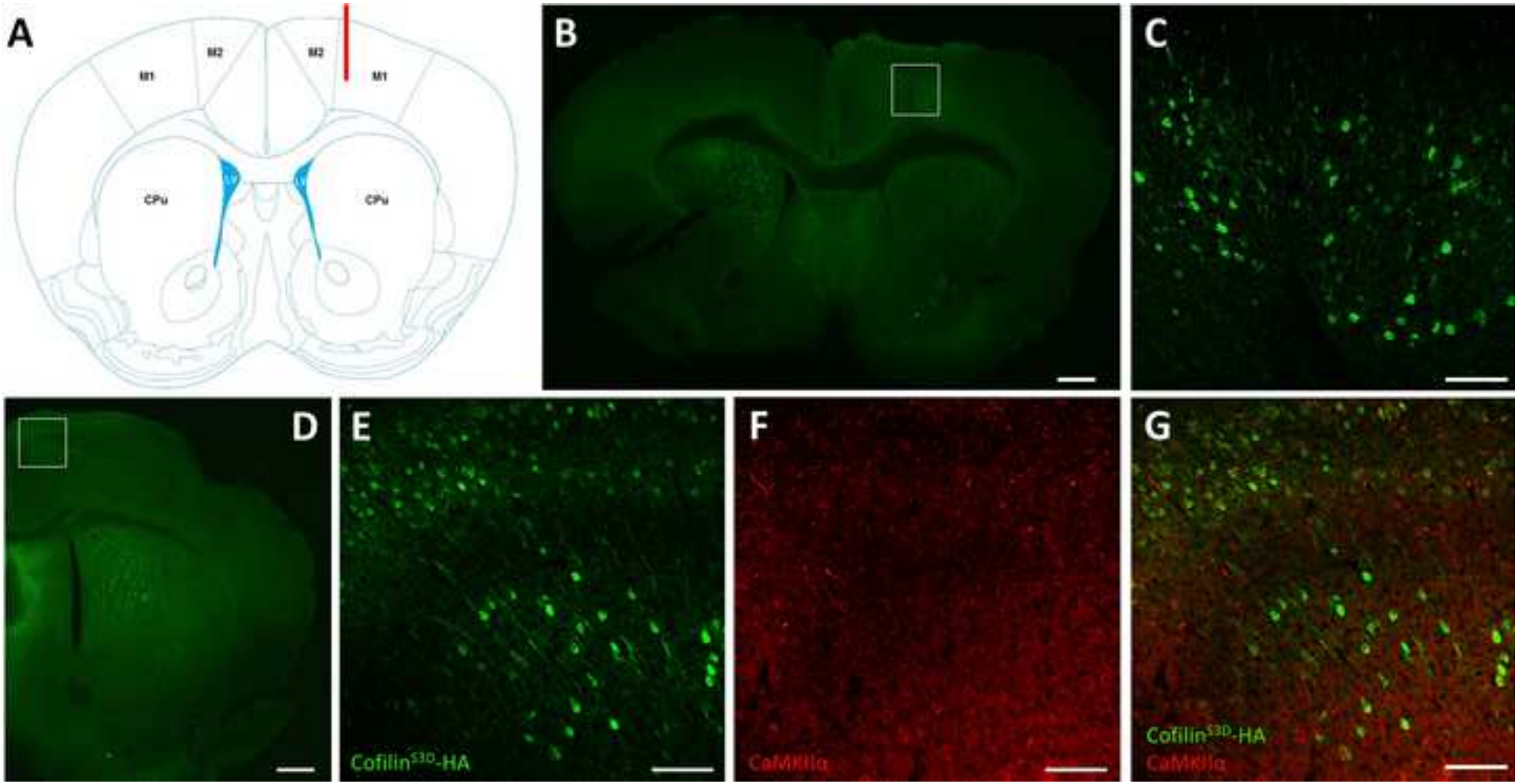

Figure 3



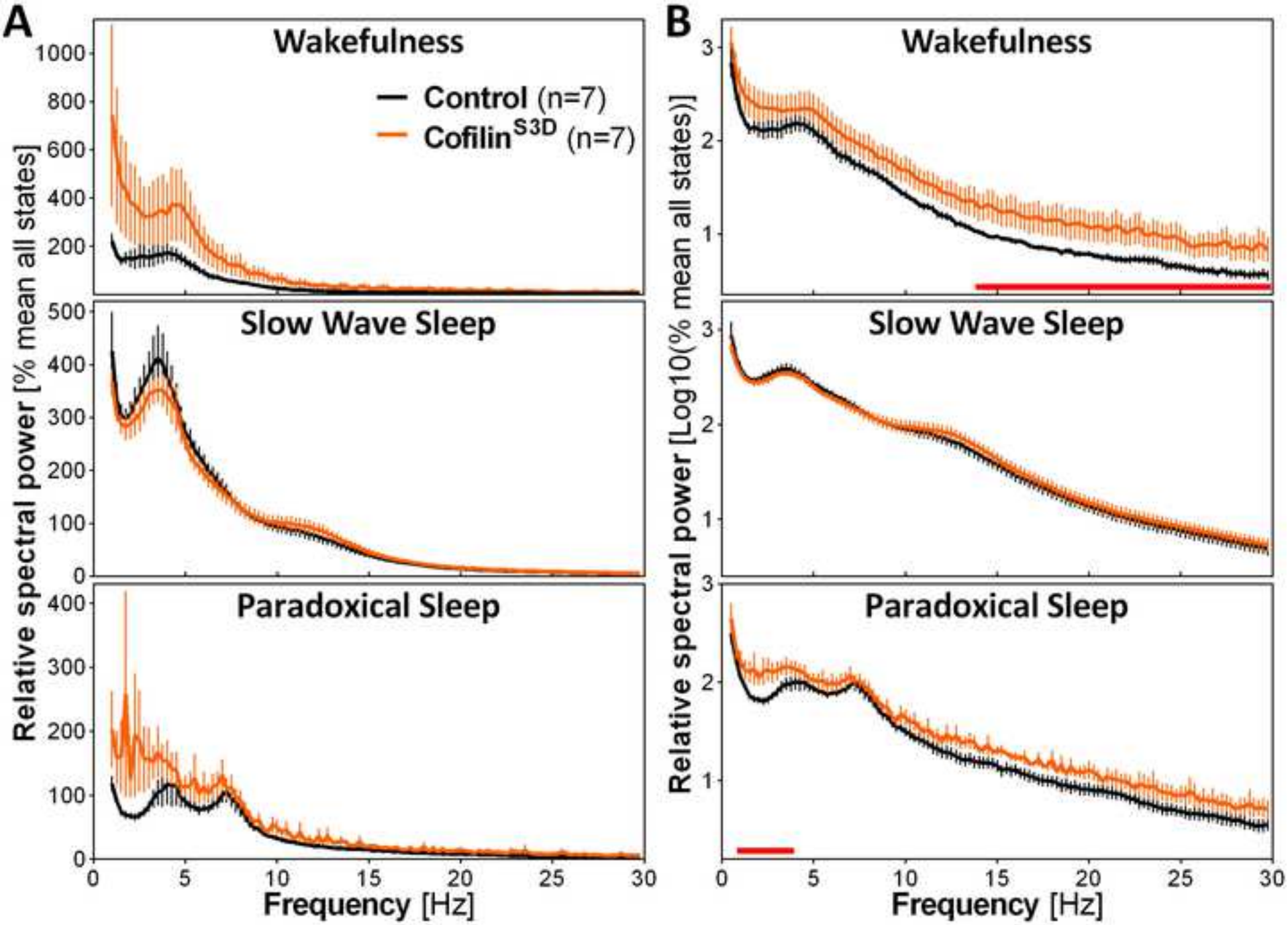

| Name of Material/Equipment/Animal | Company | Catalog Number | Comments/Description |
|---|---|---|---|
| **Surgery peparation** | | | |
| 21 G needle | Terumo | NN-2125R | |
| 6-channel connector | ENA AG | BPHF2-O6S-E-3.2 | Connector used in this manuscri |
| | Distrelec | 300-93-672 | Potential replacement for discor |
| C57BL6/J mice | Jackson Laboratory | 000664 \| B6 | Animals bred on site |
| Pluronic F-68 | | | Non-ionic surfactant |
| Gold wire 0.2 mm diameter | Delta scientific | 920-862-41 | Non-insulated |
| Hamilton syringe (10 µL) | Fisher Scientific | 14815279 | |
| Infusion syringe Pump CMA 402 | Harvard Apparatus | CMA8003110 | |
| Injection cannula 28 G | Plastics one | C313I-SPCL | |
| Isoflurane | Baxter | CA2L9100 | |
| Ketamine (10 mg/mL) | SANDOZ | 4550 | |
| Lead-free solder | AIM | SN100C | |
| Lubricating ophthalmic ointment | ALLERGAN | 210889 | |
| PE 50 Catheter thin wall | Plastics one | C232CT | |
| Flat fillister head self tapping screws | MORRIS | FF00CE125 | ECoG electrode gold covered; Di |
| Soldering iron | Weller | WES51 | |
| Syringe 1 mL | BD | 309659 | |
| Trimmer | Harvard Apparatus | 72-9063 | |
| Xylazine (20 mg/mL) | Bayer | 2169592 | |
| **Intra-cortical AAV injection with syringe pump** | | | |
| 0.7 mm drill bit | Dremel | 628 | |
| $AAV_9$-CaMKIIα0.4-cofilin$^{S3D}$-HA | UPenn Viral Core | | |
| $AAV_9$-CaMKIIα0.4-eGFP | UPenn Viral Core | | |
| Cotton tippped applicators | Medicom | 806 | |
| Drill | Dremel | 8050-N/18 | |
| Extra-fine Graefe forceps | Fine science tools | 11150-10 | |
| Stereotaxic arm | Stoelting | 51604U | |
| Stereotaxic frame | Stoelting | 51600 | |
| Surgical clamps | Fine science tools | 18050-28 | |
| Tissue scissor | Magna Stainless | M4-124 | |

| | | | |
|---|---|---|---|
| **ECoG/EMG electrode implantation** | | | |
| Buprenorphine (0.3 mg/mL) | CEVA | 57133-02 | |
| Curved forceps | Fine science tools | 11001-12 | |
| Delicate task wipers | Kimtech | 34120 | |
| Dental acrylic cement | Yates Motloid | 44115 | |
| Dumont #5 forceps | Fine science tools | 91150-20 | |
| Extra fine Graefe forceps | Fine science tools | 11150-10 | |
| Kelly forceps | Fine science tools | 13002-10 | |
| Liquid acrylic | Yates Motloid | 44119 | |
| Monocryl plus suture needle 13 mm 3/8c rev cutting | Ethicon | MCP494 | |
| Providone-iodine 10% | Triad disposables | 10-8208 | |
| RelyX Unicem 2, Adhesive Resin Cement A2 | 3M | 56849 | |
| **Immunofluorescence and ECoG recording** | | | |
| 36-Channel EEG Wearable Headbox | LaMONT Medical | 832-000350 | |
| CaMKII alpha Monoclonal Antibody (Cba-2) | Invitrogen | 13-7300 | Dilution 1:500 |
| Conductors Awg PVC Insulation Cable | Calmont Wire & Cables | HC-0819075R0 | |
| Donkey anti-Mouse IgG secondary Ab, Alexa Fluor 568 | Invitrogen | A10037 | Dilution 1:1000 |
| Goat anti-Rabbit IgG secondary Ab, Alexa Fluor 488 | Invitrogen | A-11008 | Dilution 1:500 |
| HA-Tag (C29F4) Rabbit mAb | Cell signaling | 3724 | Dilution 1:800 |
| Programmable Amplifier | LaMONT Medical | 815-000002-S2 | |
| Stellate Harmonie | Natus | HSYS-REC-LT2 | |
| Swivel connector | Crist Instrument Company Inc. | 4-TBC-9-S | |

pt, but discontinued. See potential replacement below
ıtinued connector above

mension : 1.9 mm head diameter, 1.14 mm thread major diameter, 3.6 mm length

# Response to the Reviewers' Comments

**Manuscript ID:** JoVE61976

**Title:** Electrocorticographic recording of cerebral cortex areas manipulated using an adeno-associated virus targeting cofilin in mice

**Authors:** Julien Dufort-Gervais, Robbert Havekes, Valérie Mongrain

We thank the editor and reviewers for their time and constructive comments. We have carefully revised our manuscript according to their comments, and we feel that it has been substantially improved. In brief, we have added a new figure (Figure 1) to better illustrate the preparation for surgery and some surgical steps, added several panels to previous Figures 1 and 2 (now Figures 2 and 3) to better illustrate validation procedures/analyses, applied several modifications and clarifications to the protocol, and added some important points to the discussion. The comments are repeated below followed by our detailed responses.

## Editorial comments:

1. Please take this opportunity to thoroughly proofread the manuscript to ensure that there are no spelling or grammar issues. Please use American English throughout.

RESPONSE: The manuscript has been carefully proofread to ensure that there are no spelling/grammar issues, and checked for the proper use of American English.

2. Please provide an email address for each author.

MODIFICATION: An email address is now provided for each author on the first page.

3. Please define all abbreviations at first use.

RESPONSE: The manuscript has been carefully checked to ensure that all abbreviations are defined at first use.

4. 1.2.1: what does the stock AAV mix contain?

RESPONSE AND MODIFICATION: Both the test and control AAVs are in a solution of phosphate-buffered saline (PBS) containing 0.001% Pluronic F68. This information has been added to the manuscript (step 1.2.1, page 5).

5. JoVE cannot publish manuscripts containing commercial language. This includes trademark symbols (™), registered symbols (®), and company names before an instrument or reagent. Please remove all commercial language from your manuscript and use generic terms instead. All commercial products should be sufficiently referenced in the Table of Materials and Reagents.
For example: Hamilton syringes, Relyx dental cement (3M), Stellate Harmonie (Natus), etc.

MODIFICATIONS: All commercial language has been removed, and has been replaced by generic terms as instructed.

6. 1.2.3: What is 60 cm—the tubes, length of the tube containing water?

RESPONSE AND MODIFICATION: 60 cm is indeed the length of the tube. The text has been clarified (step 1.2.3, page 5).

7. 2.4: What do you use to cut the skin?

MODIFICATION: The text now indicates that the skin is cut with a tissue scissor, and also by holding the skin with an extra fine Graefe forceps (step 2.4, page 6).

8. 2.7: How do you identify the location of the bregma and lambda?

RESPONSE AND MODIFICATIONS: The location of the bregma is identified as the intersection between the coronal and sagittal sutures of the skull, and the lambda is identified as the intersection between the skull sagittal suture and a straight line connecting the left and right lambdoid suture. This information has been added to the text (step 2.7, page 6), and is now presented in the new Figure 1D.

9. 4.2 and 4.3: How do you record ECoG/EMG signals? Please provide details to allow replication and filming (especially as you have highlighted these steps).

MODIFICATIONS: The details about the ECoG/EMG signal recording have been added to the text of the manuscript (step 4.3, page 9), together with a reference to the used equipment presented in the list of materials.

10. Please specify the euthanasia method.

MODIFICATION: The proposed use of cervical dislocation (or of other relevant methodology) is now indicated in step 4.4 (page 9).

11. Please provide more details for immunostaining: which stains and antibodies were used, how were the tissues prepared for microscopy? If these details will not be filmed, please cite a reference.

RESPONSE AND MODIFICATIONS: The primary focus of the manuscript is the injection of AAVs in a specific cortical area combined to ECoG/EMG signal recording. Immunostaining is used as a validation method, it is not the focus of the manuscript, and will not be filmed. The general methodology used for immunostaining is described in the following papers (Havekes et al., *eLife*, 2016; Tudor et al., *Sci Signal*, 2016; Evilsizor et al., *JoVE*, 2015; Dufort-Gervais et al., *Sci Rep*, 2020), which are now cited at the beginning of the section *Representative Results* (page 10). The information about the stains/antibodies is provided also in the section *Representative Results* (page 10), as well as in the legend of Figure 2 (page 11) and the attached list of materials.

12. Please ensure that the dimensions for the scale bars in Fig. 1 are visible.

RESPONSE: The dimensions of the scale bars of previous Figure 1 (now Figure 2) are indicated in the figure legend for all applicable panels (Figure 2 legend on page 11).

13. Please sort the Materials Table alphabetically by the name of the material.

MODIFICATION: The materials are now sorted alphabetically within the different sections of the attached Table as suggested.

**Reviewer #1:**

Major Concerns:
The power spectra of vigilance states seem to be very similar in shape and very different from what I and others have reported. There does not seem to be a preponderance of delta power in NREM nor a preponderance of theta power in REM sleep. In fact, for NREM, there seems to be decreased power in the middle of the delta band. Perhaps the log scale is making it difficult to differentiate, but in the case of REM there seems to be equal power in both the delta and theta bands and this should not be the case. Do the authors have an explanation? Can the data be presented in a way that preserves the spectral distributions characteristic of each vigilance state? Also, were any filters or amplification applied to the raw signal?

RESPONSE AND MODIFICATION: We politely would like to emphasize that the power spectra shown in Figure 3 are from the motor cortex (M1), which generally shows ECoG activity (or local field potential [LFP] activity) that differs considerably from the (perhaps more classical) approaches of recording above the visual cortex or of using a bipolar signal between the motor cortex and visual cortex (Funk et al., *Curr Biol*, 2016; Fernandez et al., *Cereb Cortex*, 2017). Indeed, ECoG/LFP activity in M1 is generally less different between wakefulness and slow wave sleep, and does not show a characteristic higher peak of theta activity during paradoxical sleep (Funk et al., *Curr Biol*, 2016; Fernandez et al., *Cereb Cortex*, 2017; Khlghatyan et al., *EMBO J*, 2020). Moreover, the presented slow wave sleep power spectra showing a lower power in mid-delta are comparable to previously published datasets (e.g., Freyburger et al., *Sleep*, 2016; Khlghatyan et al., *EMBO J*, 2020), and are in line with the bi-modal incidence of slow waves during slow wave sleep (Hubbard et al., *Nat Comm*, 2020). Power spectra are now newly presented in relative activity (Figure 3A), which possibly better picture differences between wakefulness and slow wave sleep in control mice, in addition to the log transformed relative activity (Figure 3B = previous Figure 2), which is more adequate to illustrate between-group differences in high frequencies. No filter was applied, and the information regarding signal amplification and sampling frequency is now provided in step 4.3 (page 9).

Minor Concerns:
Because the depth of screw electrodes is an important variable, it would be useful to have detailed description, including length from the screw head, of these screws; this detail would allow substitution of similar screws if so desired.

RESPONSE AND MODIFICATIONS: We thank the reviewer for the suggestion. The dimensions of the screws have been added to the legend of new Figure 1 showing a prepared screw for surgical implantation (page 11), and to the attached list of materials.

Along with these same lines, can the authors provide an estimate of the final screw depth using the skull surface as a reference?

MODIFICATION: An estimate of the final screw depth is now provided in the revised text of the manuscript (step 3.1, page 7).

Lead-free solder is best for these applications, I suggest this term be used in place of soldering lead.

MODIFICATIONS: The term soldering lead was replaced by lead-free solder throughout the manuscript (i.e., pages 5 and 11), as well as in the attached list of materials.

The term "6-channel plastic box" is vague and I was unable to find the vendor (ENA AG) or product (BPHF2-O6S-E-3.2) with a google search. Could more detail on the vendor be provided?

RESPONSE AND MODIFICATIONS: This specific connector is unfortunately discontinued, and we thank the reviewer for his vigilance in this regards. We have added a potential replacement to the list of materials (i.e., Distrelec, article no. 300-93-672). The term ''6-channel plastic box'' has been replaced by ''6-channel connector'' (page 5), and a picture of the connector is newly shown in Figure 1C.

The use of a multimeter with the ability to confirm continuity should be suggested as a means to detect bad connection during the procedure.

RESPONSE: The use of a multimeter is particularly desirable to assess the integrity and suitability of recording cables and swivel connectors. With regards to the surgery, a multimeter could be used only to detect unwanted connections between electrodes, as indicated by the reviewer, by testing all combinations of electrodes (i.e., 25 combinations for 5 electrodes). We believe this addition would slow down the surgery process too much, and would not necessarily be superior to the careful visual examination of electrodes and of their solders.

**Reviewer #2:**

Major Concerns:
The immunohistochemical verification of the injection site is not convincing/of sufficient quality. As one of the major parts of the suggested methodology is precise brain area and/or cell-specific AAV manipulation, I would strongly recommend the authors to describe steps on how to perform appropriate controls to confirm such specificity in their protocol, and also address it in their own representative results in figure 1.
a. It is not clear in figure 1 which area has been infected with the AAV. I would encourage the authors to provide better quality and more detailed immunohistochemical images to strengthen the validity of their method. The highest fluorescence it seems is seen in the left subcortical area and not in the

motor cortex. The authors comment that it might be due to projections to distant brain areas, however it is unclear from the provided image whether the labelling on contralateral subcortical area is axonal or somatic.

RESPONSE AND MODIFICATIONS: The quality of the immunohistochemistry figure (previous Figure 1, current Figure 2) is adequate in the image format submitted (i.e., jpeg), but we agree that it is not sufficient in the merged pdf document (generated by the submission website for the review process) that combines the text with figures. We thus invite the reviewer to look at the original submitted image that should be separately accessible from the website. The panel B and the new panel D clearly show stained cell bodies in the cerebral cortex (M1 and M2), which are particularly evident in higher magnification panels C and E. The subcortical staining observed in the striatum (and particularly intense in the contralateral hemisphere) appears to localize to myelinated axon fibers (see adjacent higher magnification picture). This agrees with the known projections from the motor cortex to the caudate putamen (e.g., Guo et al., *PLoS One*, 2015). We prefer not to include this image given that a characterization of cortical projections to the striatum is out of the scope of the present manuscript.

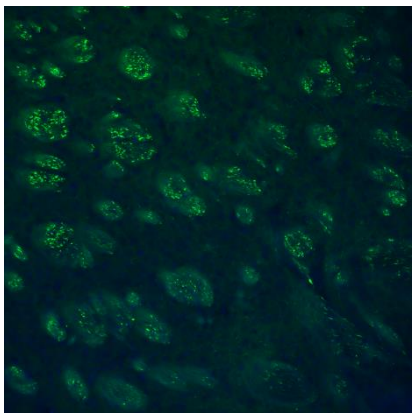

b. Moreover, immunostaining for the infected AAV should be done with co-staining of a known marker for the targeted cell type (for example NeuN for neurons) to show that the expected cells were successfully targeted. The authors mention this themselves "Co-staining with markers of excitatory neurons (e.g., vGlut1) could also be performed to validate cell type specificity" and I would strongly recommend to do so, and also add it as a step in their protocol.

MODIFICATIONS AND RESPONSE: Co-staining of cofilin$^{S3D}$-HA and CaMKII$\alpha$ (of which the promotor was used to drive the expression of cofilin$^{S3D}$-HA) has now been included in the *Representative Results* (pages 10 and 11), and is featured in the new panels F and G of Figure 2. This co-staining indeed helps to validate the targeting of excitatory neurons with the AAV. However, as indicated above in the response to the editorial comment #11, immunostaining is used as a validation method and is not the primary focus of the manuscript, and we thus prefer not to include it in the description of the main protocol. We have now cited a paper published in *JoVE* that specifically focuses on the procedures for proper immunohistochemistry (Evilsizor et al., *JoVE*, 2015).

c. Also, as the method strongly depends on the specificity of the AAV infecting the expected cells, the authors could also encourage future protocol users to evaluate viral transfection specificity (how many non-targeted cells were infected? E.g. if excitatory neurons were targeted, do you see inhibitory neuron/microglial/astrocyte labelling?) and efficacy (how many of the targeted cell type were infected with the construct in question - for example how many of the vGlut1stained excitatory neurons were also positive for the cofilinS3D-HA?).

MODIFICATION AND RESPONSE: The discussion (page 14) now directly encourages future protocol users to assess the efficacy of viral infection by calculating, on co-staining higher magnification images, the percent target cells successfully infected by the AAV (e.g., number of cells showing

double-labeling out of the total number of cells showing single labeling of the target, here CaMKIIα expressing neurons). We would like to point out that the use of cell type-specific promoters is common practice for the generation of cell type-specific transgenic mice and to guide the expression of transgenes using viral approaches. In case of AAVs, using a *CamKII* promoter fragment, we have previously shown that expression is restricted to excitatory neurons with no expression in, for example, interneurons or astrocytes (e.g., Havekes et al., *eLife*, 2016; Tudor et al., *Sci Signal*, 2016).

d. Moreover, authors might consider adding to their protocol the evaluation of reactive gliosis and microglia activation in the injection site as this might also alter neuronal network properties and hence ECoG readout.

RESPONSE AND MODIFICATION: We feel that it is important to underline that our AAV-ECoG protocol highlights the importance of conducting experiments in control groups simultaneously to test groups (pages 5, 13, and 14). Accordingly, reactive gliosis and microglia activation that could take place as a function of the surgery are expected to be similar in the two groups, and thus to be controlled for in their potential effect on the neuronal network and ECoG activity. We have added a note in this regards in the paragraph describing limitations in the discussion (page 14).

Minor Concerns:
ECoG and EMG electrode preparation and implantation requires a more detailed description:
a. For example, even though I assume that the ECoG golden wire should be soldered onto the very top of the screw cap to later be soldered to the connector, I think that should be clearly mentioned in the protocol, because some ECoG electrodes are made so that the wire actually goes into the brain and I am afraid might create confusion.

MODIFICATIONS: This clarification has been added to the text (step 1.1.1, page 5), and is also featured in the new Figure 1A.

I would recommend to use photographs/illustrations of how the prepared electrodes should look like and several images or at least a final image on how the implanted electrodes should look like (before soldering the connector on).

MODIFICATIONS: We thank the reviewer for this suggestion and a new figure (Figure 1) now illustrates these components, with, in particular, panel A showing an ECoG electrode before implantation, panel B showing EMG electrodes before implantation, and panel D showing the implanted ECoG electrodes and anchor screws.

b. What are maintenance screws (mentioned in 2.8)? Reference electrodes?

RESPONSE AND MODIFICATION: Maintenance screws are regular screws (not covered with gold) that are screwed on the skull (of the left hemisphere), and that are required to ensure a robust montage. The adherence of cement to these (additional) screws acts as a solid anchor on the skull. They are not soldered to the connector. A precision has been added to this text now presented at step 3.2 (page 8).

c. How exactly do the authors insert the EMG electrodes into the muscle? Wouldn't the 0.2 mm wire would bend when bluntly forced into the muscle?

RESPONSE AND MODIFICATIONS: EMG electrodes are inserted in the muscle by gently pushing the extremity of the gold wire in the muscle with Dumont #5 forceps. During this process, the skin is lifted with extra fine Graefe forceps, and very little resistance occurs. The small diameter of the wire likely facilitates the insertion in the muscle. Clarifications have been added to step 3.6 (page 8).

d. The authors do not comment whether the wire used for both ECoG and EMG electrodes is insulated or not. I would assume that soldering process would remove the insulation, but do the authors treat the end of the EMG electrode that is inserted into the muscle?

RESPONSE AND MODIFICATIONS: The gold wire used for ECoG and EMG electrodes is non-insulated. The cement acts as the insulator when the montage is completed. This information that the gold wire is non-insulated has been added to the manuscript (step 1.1.1, page 5; legend of Figure 1) and the attached list of materials.

e. Do the authors always recommend to use same burr holes for AAV injection and ECoG electrode implantation? How should one adjust the position of the other 2 ECoG electrodes depending where the AAV injection will take place? Is it possible with this methodology to inject AAV using a burr hole that afterwards is not used for ECoG implantation? If yes - how should one close up the burr hole? I would like to see some more specific comment on this topic.

MODIFICATION: The suggestion of performing AAV injection in a site different from the ECoG recording sites has been included in the discussion, together with a strategy to cover the burr hole not used for ECoG recording (top of page 14).

f. I would suggest to add the comment "(i.e., seeing two screw crests and roots)" not to the discussion as is now, but to the protocol itself (step 3.1)

MODIFICATION: Step 3.1 has been modified with the more quantitative measure of screw length out of the skull (page 7).

More minor points

1. A comment on the depth of injections: "Align the cannula with the anterior hole on the skull in order for the vertical position of the cannula to reach the upper edge of the skull (i.e., skull surface)." As the thickness of the skull of mice may vary according to gender and age, measuring form the cortical surface could be regarded as more accurate.

RESPONSE AND MODIFICATION: We agree that measuring the depth of injection from the cortical surface could be more accurate. However, in practice, the small size of the burr hole makes it impossible to clearly visually identify the cortical surface. In addition, the stereotaxic coordinates used in the present protocol (steps 2.8 and 2.13) are based on the book *The mouse brain in stereotaxic coordinates* (Franklin and Paxinos; see new reference #40 in the manuscript), which uses the skull surface as a reference. The information that skull thickness varies with age and sex (the notion of gender does not apply in mice) and that the position of the cannula should be verified

with post-protocol histology/immunohistochemistry have been added to the first paragraph of the discussion (page 13).

2. Why are animals housed in individual cages? If possible avoiding single housing would be better, even though this typically prevent usage of certain materials.

RESPONSE AND MODIFICATION: Animals are housed individually to avoid damage to the head montage, and to prevent damage/entanglement of the recording cables, as group housed mice tend to damage the cables and head montage while grooming one another. This information has been added to the text of the manuscript (step 4.1, page 9).

3. To be on the safe side, ophthalmic ointment should probably be applied immediately after the anesthesia sets in.

RESPONSE: The application of ointment is preferred after mouse shaving in order not to interfere with the hair trimmer function, and to avoid hair sticking on the ointment. This step is relatively quick and is not contributing to eye dryness in our hands.

4. In 2.6. might be better to scrape the periosteum with a scalpel rather than scissors. Also - edging vertical and horizontal lines with a scalpel blade and making a checker board pattern helps to hold the implant in place even more.

RESPONSE AND MODIFICATION: The scissor tip works very well in our hands as will be demonstrated in the video. Step 2.6 has been modified to emphasize the need to create streaks in different directions (page 6).

5. Is 10% betadine solution suitable for internal use (mentioned in 2.9)? And would it not be a risk for fluid entering the burr holes?

RESPONSE: The amount of 10% betadine solution (changed for providone-iodine to avoid commercial names) used to disinfect the skull after piercing is minimal because impregnated in the cotton tip, and it is thus not significantly entering in the burr holes. In any case, this antiseptic solution should not do any harm to mice as any excess will be absorbed by the small rolled pieces of delicate task wipers used in step 3.3.

6. After inserting the cannula into desired depth I would recommend to wait quite some time (20 min?) for the insertion tract to close and avoid backflow.

RESPONSE: Given that the surgery should be conducted as quickly as possible to ensure stable anesthesia throughout the procedure, we do not recommend waiting before injection after the insertion of the cannula. In addition, backflow is importantly minimized by the long injection time (i.e., 40 min) and the 5 min waiting time after the end of the injection.

7. Could authors expand on what they mean by "if required" mentioned in 3.16 as to whether administer painkiller 12 h after the surgery.

MODIFICATION: The information of providing additional painkiller if the animal is showing signs of pain 12 h after the surgery has been added to this step (now 3.17, page 9).

8. Do authors recommend or have any comments whether there could be recordings performed in several consecutive days? How long does the implant and the recordings remain good quality?

MODIFICATION: The information that the recording can be performed for several consecutive days has been added to the second paragraph of the discussion (page 13).

Text edits

1. Homogenize the use of either "EEG" or "ECoG"
2. Correct spelling of Hamilton syringe in the material table

MODIFICATIONS: These changes have been applied.

**REFERENCE cited only in this Response to the Reviewers' Comments (other references cited are provided in the reference list of the manuscript)**

Fernandez, L.M.J., *et al*. Highly dynamic spatiotemporal organization of low-frequency activities during behavioral states in the mouse cerebral cortex. *Cerebral Cortex*. **27** (12), 5444-5462 (2017).

Funk, C.M., Honjoh, S., Rodriguez, A.V., Cirelli, C., Tononi, G. Local slow waves in superficial layers of primary cortical areas during REM Sleep. *Current Biology*. **26** (3), 396-403 (2016).

Guo, Q., *et al*. Whole-brain mapping of inputs to projection neurons and cholinergic interneurons in the dorsal striatum. *PLoS One*. **10** (4), e0123381 (2015).